1111

Theoretical Aspects of Photoinitiated Chemisorption, Dissociation, and Desorption of O_2 on Pt(111)

A. W. Edith Chan,[†] Roald Hoffmann,*,[†] and W. Ho[‡]

Departments of Chemistry and Physics and Materials Science Center, Cornell University,
Ithaca, New York 14853

The chemisorption of molecular oxygen on a Pt(111) surface of a three layer slab model is examined using tight-binding extended Hückel calculations. On-top, 2-fold-bridge, and 3-fold-capped sites are considered. Chemisorption of O_2 appears to be more favorable at the 2-fold site. The stabilization is due to the better overlap of the O_2 $2\sigma_u$ orbital with the Pt surface. Photoinitiated dissociation and desorption mechanisms of O_2 are studied using an extended surface and a cluster model. Dissociation begins by stretching the O–O bond as the O_2 π^* becomes occupied via electronic excitation. This results in a lowering in energy of the O_2 σ^*, which is subsequently filled partially by electrons. Desorption is attributed to a π^*_z(Pt–O) to π^*_z(Pt–O)* excitation. Photodesorption and photodissociation of O_2 on Pt(111) proceed via direct excitation of the adsorbate–substrate complex.

Introduction

Recently the ultraviolet photolysis of simple molecules chemisorbed on single-crystal metal surfaces has been achieved.[1] Experiments have been done with different adsorbates, e.g. O_2, on various surfaces, including Ni, Pt, and Pd.[1,2] A number of mechanisms have been identified to explain the observed photoinitiated processes. In one such mechanism, a single UV photon with energy comparable to that of a chemical bond can be taken up by an adsorbate, and the excited molecule may then dissociate or desorb before the excitation is quenched by the metal.

Mieher and Ho[3] have reported on the photodissociation of O_2 molecule and the coadsorption of O_2 with CO[3a] and NO[3b] on Pt(111). There were some differences in the outcome of these two experiments. In the CO case, the authors concluded that photoabsorption by the O_2–substrate complex causes an optical transition from the ground state to an electronically excited state; O_2 then photodissociates into two "hot" oxygen atoms. The formation of CO_2 is attributed to the collision of a "hot" oxygen atom with coadsorbed CO. However, in the NO case, a new adsorbed state, γ-NO, with significantly enhanced photodesorption cross section, was detected on the surface. Although NO_2 production was not reported,[3b] further studies have shown that irradiation of O_2 coadsorbed with NO also leads to the formation of NO_2 through the "hot" oxygen atom mechanism.[4]

In another contribution by Zhu, Hatch, Campion, and White,[2b] three kinds of photoinduced reactions of O_2 on Pt(111) were characterized by high-resolution electron energy loss spectroscopy (EELS) and temperature programmed desorption (TPD). These reactions are photoinduced dissociation, desorption, and rearrangement. In addition, the mechanism for dissociation involves a π^*_y to π^*_z(Pt–O)* (this notation will be explained later in the text) intramolecular transition, and that of desorption a π^*_y to σ^* transition.

There are two dominant excitations which might be initiated by photoabsorption:[1,5,6] (1) excitation of substrate electrons followed by electron (or hole) attachment to the adsorbate–substrate complex (the hot carrier effect); (2) direct excitation of adsorbate–substrate complex. Solid surfaces play additional roles in surface photochemistry. Surfaces can provide many efficient channels for quenching the excitations. Depending on the nature of the interaction with the surface, many symmetry restrictions may be removed when the molecule is adsorbed, thus influencing the selection rules for photoexcitation. For example, an electronic excitation from σ_g to π_u of the O_2 molecule in gas phase is not dipole-allowed. However, when the molecule is chemisorbed in the on-top site on Pt(111), this transition becomes allowed, because the local point group symmetry of the composite system is C_{2v}. We will comment on this in a later section.

In this report, the focus will be on both conventional chemisorption and dynamical phenomena. We hope to provide mechanistic suggestions for the photon-driven chemical processes, which involve the making and breaking of bonds at adsorbate–metal interfaces. The extended Hückel tight-binding method[7] will be used to examine the system. This procedure is an approximate molecular orbital (MO) method with well-known deficiencies. For instance, it does not give reliable potential energy curves. But it is a transparent methodology and reveals clearly the basic interactions that are responsible for bonding.[8] The tools we use are density of states (DOS) analysis, including local or projected DOS contributions, crystal

---

(1) (a) Chuang, T. J. Surf. Sci. Rep. 1983, 3, 1. (b) Ho, W. In Desorption Induced by Electronic Transitions, DIET IV; Betz, G., Varga, P., Eds.; Springer Series in Surface Science; Springer-Verlag: Secaucus, NJ, 1990; Vol. 19, p 48, and refs 1–5 therein. (c) Polanyi, J. C.; Rieley, H. In Dynamics of Gas-Surface Interactions; Rettner, C. T., Ashfold, M. N. R., Eds.; Royal Society of Chemistry: London, 1991; Chapter 8. (d) Zhou, X.-L.; Zhu, X.-Y.; White, J. M. Submitted for publication in Surf. Sci. Rep.
(2) (a) Guo, X.; Hanley, L.; Yates, J. T., Jr. J. Chem. Phys. 1989, 90, 5200; J. Chem. Phys. 1989, 91, 7220. (b) Zhu, X.-Y.; Hatch, S. R.; Campion, A.; White, J. M. J. Chem. Phys. 1989, 91, 5011. (c) Yoshinobu, J.; Guo, X.; Yates, J. T., Jr. J. Chem. Phys. Lett. 1990, 169, 209; Vac. Sci. Technol. A, in press. (d) White, J. M.; Hatch, S.; Zhou, X.-Y.; Campion, A. Vacuum 1990, 41, 282. (e) Hatch, S.; Zhu, X.-Y.; White, J. M.; Campion, A. J. Chem. Phys. 1990, 91, 2681; J. Phys. Chem. 1991, 95, 1759. (f) Wolf, M.; Nettesheim, S.; White, J. M.; Hasselbrink, E.; Ertl, G. J. Chem. Phys. 1990, 92, 1509; submitted for publication in Surf. Sci.
(3) (a) Mieher, W. D.; Ho, W. J. Chem. Phys. 1989, 91, 2755; work to be submitted for publication. (b) Mieher, W. D.; Ho, W. J. Chem. Phys. 1990, 92, 5162.
(4) Mieher, W. D.; Pelak, R. A.; Ho, W. To be submitted for publication.

(5) Avouris, P.; Walkup, R. E. Annu. Rev. Phys. Chem. 1989, 40, 173.
(6) Zhou, X.-L.; Zhu, X.-Y.; White, J. M. Acc. Chem. Res. 1990, 23, 327.
(7) For a description of the methodology and the use of these indices in tracing down orbital interactions, see Hoffmann, R. In Solids and Surfaces: A Chemist's View in Bonding in Extended Structures; VCH: New York, 1988.
(8) Zonnevylle, M. C.; Hoffmann, R. Langmuir 1987, 3, 452.

orbital overlap populations (COOP), and overlap populations (OP).[7] A fragment analysis allows us to compare the changes between the bare surface, the adsorbate, and the composite chemisorbed system. Additional computational information is discussed in the Appendix.

Our aim is to determine the relative strengths of the O_2–Pt interaction in different adsorption sites and to identify those states which are most likely to lead to the following reactions: (1) dissociation of O_2, followed by migration of O atom; (2) bond weakening of Pt–O, leading to desorption of O_2. If there is an excitation, we would like to be able to predict whether the dioxygen in this site will dissociate or desorb.
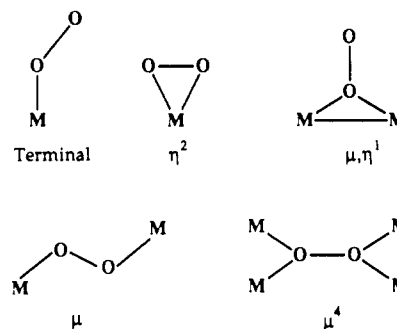
Discussions of dissociation reactions have centered on the extent of electron transfer into the π^* orbital of O_2. The more electrons in the π^*, the weaker that bond. The O–O overlap population may serve as an important index of incipient dissociation. The precise coordination mode to a Pt(111) surface should certainly influence the course of the subsequent reaction. An indicator of a desorption reaction might be Pt–O bond weakening, accompanied by a small change in the O–O bond strength.

Oxygen adsorbed on Pt(111) has been extensively studied by various experimental techniques.[2,3,9] Below 30 K, O_2 is physisorbed on the surface.[9a,b] Gland and coworkers have investigated this system with TPD, low-energy electron diffraction (LEED), ultraviolet photoelectron spectroscopy (UPS), and EELS. The adsorption of oxygen molecules is commonly carried out at 100 K. Around 150 K, some of the O_2 desorb molecularly and some dissociate into adsorbed atomic oxygen, occupying only the 3-fold site, which then desorb at 600 K. Both EELS and near-edge X-ray-absorption fine-structure (NEXAFS) data support a stretched O–O bond parallel to the surface, the molecule adsorbed in a π-bonded configuration. The lengthening of the O–O bond is due to the electron transfer into the antibonding π_g level. $\pi^*_\perp$ (π^*_z, z axis perpendicular to surface) is broadened due to its involvement in the chemisorption while $\pi^*_\parallel$ (π^*_y, y axis parallel to surface) is unperturbed.

An ordered overlayer structure is usually hard to observe,[9a,b] due to the system's sensitivity to the electron beam. However, an ordered structure was observed with LEED[9l] in a $(3/2 \times 3/2)R15°$ cell with coverage = 0.44 of a monolayer (ML). In general, the saturation coverage is around 0.44–0.5 ML. EELS spectra show two O–O loss peaks: around 860–870 (usually assigned to an atop species) and 690–700 cm^{-1}. The intensity of the former peak increases monotonically with coverage, while the latter one decreases in intensity with the coverage. At low coverages ($\theta < 0.25$ ML), the lower frequency peak is more intense, while at higher coverages, the higher frequency peak becomes more intense. Two explanations were forwarded,[9] one being that there are two adsorption sites, and the other that adsorption involves a step or defect site.

Chart I

The bond order of an oxygen molecule adsorbed on surfaces has been the subject of experimental controversy. On Pt(111), the bond order was estimated to be 1.0 (corresponding to a bond length = 1.45 Å), a peroxide type. Recently, with a more accurate method, NEXAFS, the O–O bond order was estimated to be 1.5 (corresponding to a bond length = 1.32 Å), a superoxide instead.[9h,j] A more recent work by the same group re-evaluated their data and estimated a bond length of 1.37 Å[9l] instead. Extended Hückel calculations were repeated at this value, and the trend of the results and the conclusion between these two values are the same. An O–O bond distance of 1.32 Å[9h] will be used in this study. Valence-level photoemission studies indicated that the π_g (π^*) level was at least partially filled. This fact and the increase in the work function of 0.8 eV upon O_2 adsorption were taken as evidence of stretching of the O–O bond.

A number of theoretical calculations have been done on O_2 on a Ag surface,[10a-f] Pt(111),[10g] and Ni(100).[10h] Panas, Siegbahn, and Wahlgren[10g,h] suggest that the dissociation mechanism over the different sites is essentially the same, even though the energetics differ. They proposed that the dissociation of O_2 on Ni(00) went through a $\pi_{gy} \leftarrow \pi_{uz}$ excitation and that metal d orbitals did not participate much in the bonding. Their conclusion in the Pt(111) study[10g] was that O_2 generally adsorbs in the 2-fold-bridge site, with the O–O bond parallel to the surface. There is also extensive electron transfer from the surface at the equilibrium geometry.

Pt–Dioxygen Organometallic Compounds

Usually the Pt–O bond length in organometallic molecules is around 1.9–2.0 Å.[11] Dioxygen coordinates in many ways with metals in discrete molecules:[12] terminal, η^2, μ, μ^4,[13] and even μ,η^1 (only with Al[14]). These geometries are shown in Chart I The O–O distance usually ranges from 1.2 to 1.3 Å for terminal dioxygen, 1.46 and 1.48 Å for η^2 and μ type, respectively. In comparison, the bond length for gas-phase dioxygen is 1.208 Å.[11b] The η^2 complexes,

(9) (a) Gland, J. L. *Surf. Sci.* **1980**, *93*, 487. (b) Gland, J. L.; Sexton, B. A.; Fisher, G. B. *Surf. Sci.* **1980**, *95*, 587. (c) Fisher, G. B.; Sexton, B. A.; Gland, J. L. *J. Vac. Sci. Technol.* **1980**, *17*, 144. (d) Gland, J. L.; Gland, J. L.; Eberhardt, W.; Outka, D. A.; Madix, R. J.; Sette, F.; Koestner, R. I.; Doebler, U. *Phys. Rev. Lett.* **1983**, *51*, 2414. (e) Steininger, H.; Lehwald, S.; Ibach, H. *Surf. Sci.* **1982**, *123*, 1. (f) Avery, N. R. *Chem. Phys. Lett.* **1983**, *96*, 371. (g) Derry, G. N.; Ross, P. N. *J. Chem. Phys.* **1985**, *82*, 2772. (h) Outka, D. A.; Stöhr, J.; Jark, W.; Stevens, P.; Solomon, J.; Madix, R. J. *Phys. Rev. B: Condens. Matter* **1987**, *35*, 4119. (i) Winkler, A.; Guo, X.; Siddiqui, H. R.; Hagans, P. L.; Yates, J. T. *Surf. Sci.* **1988**, *201*, 419. (j) Eberhardt, W.; Upton, T.; Cramm, S.; Incoccia, L. *Chem. Phys. Lett.* **1988**, *146*, 561. (k) Eberhardt, W.; Upton, T.; Cramm, S.; Incoccia, L. *J. Vac. Sci. Technol., A* **1988**, *6*, 876. (l) Wurth, W.; Stöhr, J.; Feulner, P.; Pan, X.; Bauchspiess, K. R.; Baba, Y.; Hudel, E.; Menzel, D. *Phys. Rev. Lett.* **1990**, *65*, 2426. (m) Norton, P. R. *Surf. Sci.* **1975**, *47*, 98.

(10) (a) Lin, J.-H.; Garrison, B. J. *J. Chem. Phys.* **1984**, *80*, 2904. (b) Selmani, A.; Sichel, J. M.; Salahub, D. R. *Surf. Sci.* **1985**, *157*, 208. (c) Selmani, A.; Andzelm, J.; Salahub, D. R. *Int. J. Quantum Chem.* **1986**, *29*, 829. (d) Upton, T. H.; Stevens, P.; Madix, R. J. *J. Chem. Phys.* **1988**, *88*, 3988. (e) Zonnevylle, M. C.; Van den Hoeck, P. J.; Van Santen, R. A.; Hoffmann, R. *Surf. Sci.* **1989**, *223*, 233. (f) Jørgensen, K. A.; Hoffmann, R. *J. Phys. Chem.* **1990**, *94*, 3046. (g) Panas, I.; Siegbahn, P. *Chem. Phys. Lett.* **1988**, *88*, 458. (h) Panas, I.; Siegbahn, P.; Wahlgren, U. *J. Chem. Phys.* **1989**, *90*, 6791.

(11) (a) Orpen, A. G.; Brammer, L.; Allen, F. H.; Kennard, O.; Watson, D. G.; Taylor, R. *J. Chem. Soc., Dalton Trans.* **1989**, S1. (b) Greenwood, N. N.; Earnshaw, A. In *Chemistry of the Elements*; Pergamon Press: Oxford, 1984.

(12) Gubelmann, M. H.; Williams, A. F. *Struct. Bonding* **1983**, *55*, 1.

(13) (a) Micklitz, W.; Bott, S. G.; Bentsen, J. G.; Lippard, S. J. *J. Am. Chem. Soc.* **1989**, *111*, 372. (b) Stibrany, R. T.; Gorum, S. M. *Angew. Chem., Int. Ed. Engl.* **1990**, *29*, 1156.
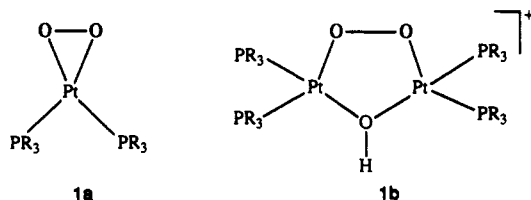
(14) Hrncir, D. C.; Rogers, R. D.; Atwood, J. L. *J. Am. Chem. Soc.* **1981**, *103*, 4277.

Table I. Calculated Overlap Populations (OP) for Some Pt-O₂ Complexes

	O–O, Å	O–O (OP)	Pt–O (OP)
PtO₂(PH₃)₂	1.32	0.51	0.20
	1.43	0.42	0.21
	1.50	0.37	0.22
Pt₂O₂(OH)(PH₃)₄⁺	1.32	0.45	0.30
	1.54	0.30	0.29

which are also called Vaska-type compounds, are by far the most widespread among the transition metals, while the μ complexes are less common. In all cases, complex formation is accompanied by a significant increase in the O–O interatomic distance and a considerable decrease in the O–O vibrational stretching frequency (ν(O–O)).

There are a few Vaska-type Pt compounds (Pt(O₂)-[(PR₃)]₂, 2a);[15] the O–O distances in these are found to be around 1.43 and 1.50 Å. The Pt–O distance is around 2.0 Å. To probe the bonding in these compounds, extended Hückel calculations were carried out on a model compound, Pt(O₂)(PH₃)₂[16] (1a). The Pt–O bond length is set to 2.0 Å. Three different O–O bond distances have been used: 1.32, 1.43, and 1.50 Å. The first distance is the experimental value obtained from the chemisorption of O₂ on Pt(111).[9h] The other two are from the discrete molecules mentioned above. The Pt–O and O–O overlap populations are listed in Table I.

```
     O—O                  O————O          +
      \ /            PR₃\  |    |  /PR₃
       Pt               Pt        Pt
      /  \            PR₃/  \  /  \PR₃
   PR₃    PR₃                 O
                              |
                              H

      1a                      1b
```

Another compound, [Pt₂(O₂)(OH)(PR₃)₄][ClO₄]·2C₆H₆[17] (1b) resembles a 2-fold (on a surface) adsorbed O₂. Calculations were carried out on the compound 1b, setting the Pt–O distance to 2.0 Å. The O–O distances were set to the experimental value of this compound, 1.54 Å, and the value from O₂ chemisorption on Pt(111), 1.32 Å.[9h] The calculated overlap populations are also listed in Table I. When the dioxygen coordinates to one Pt, the Pt–O bond is weaker. Roughly, the Pt–O overlap population (OP) is approximately 0.2 when the oxygen is bound with one Pt, and approximately 0.3 when it is bonded to two Pt atoms. The Pt–O distance will be taken as 2.0 Å in this study. The O–O OP decreases as a function of O–O distance, indicating electrons filling the π* orbitals.

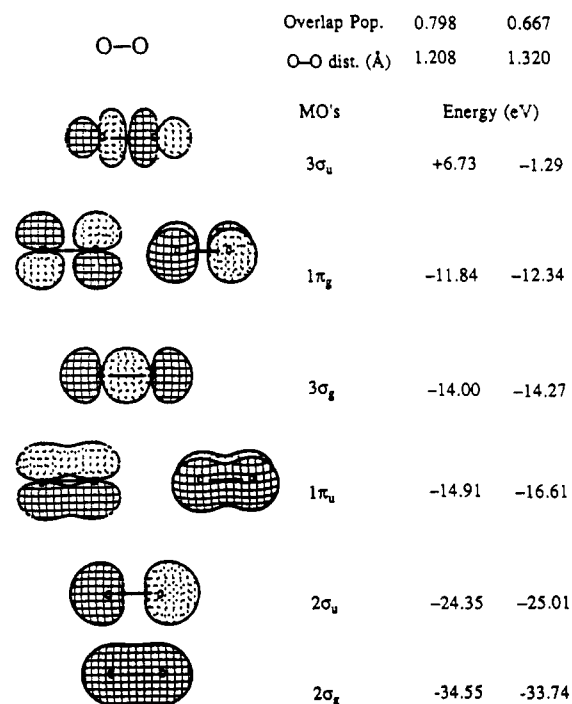## Pt(111) Surface and O₂ Molecule

Pt(111) is a hexagonal surface with a nearest neighbor distance of 2.77 Å.[18] A three-layer slab of Pt(111) was chosen to model the substrate; this slab thickness has been previously shown to be a fair compromise between realistic

(15) (a) Kashiwagi, T.; Yasuoka, N.; Kasai, N.; Kakudo, M.; Takahashi, S.; Wagihara, N. *J. Chem. Soc. D* **1969**, 743. (b) Cook, C. D.; Cheng, P.-T.; Nyburg, S. C. *J. Am. Chem. Soc.* **1969**, *91*, 2123. (c) Cheng, P.-T.; Cook, C. D.; Nyburg, S. C.; Wan, K. Y. *Can. J. Chem.* **1971**, *49*, 3772. (d) Yoshida, T.; Tatsumi, K.; Matsumoto, M.; Nakatsu, K.; Nakamura, A.; Fueno, T.; Otsuka, S. *Nouv. J. Chim.* **1979**, *3*, 761.
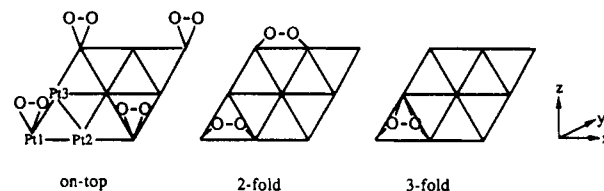
(16) Norman, J. G. *Inorg. Chem.* **1977**, *16*, 1328. The results of the SCF-Xα-SW calculations by Norman done on the model compound, Pt-(O₂)(PH₃)₂ (O–O and Pt–O are 1.50 and 2.00 Å, respectively) were similar to ours.

(17) Bahaduri, S.; Casella, L.; Ugo, R.; Raithby, P.; Zuccaro, C.; Hursthouse, M. *J. Chem. Soc., Dalton Trans.* **1979**, 1624.

(18) Kittel, C. *Introduction to Solid State Physics*; John Wiley & Sons: New York, 1986.

Overlap Pop.	0.798	0.667
O–O dist. (Å)	1.208	1.320

MO's	Energy (eV)	
3σᵤ	+6.73	–1.29
1πₛ	–11.84	–12.34
3σₛ	–14.00	–14.27
1πᵤ	–14.91	–16.61
2σᵤ	–24.35	–25.01
2σₛ	–34.55	–33.74

Figure 1. Molecular orbital diagram of a free O₂ molecule.

Chart II

on-top   2-fold   3-fold

modeling and computational economy.[19] The overlap populations of the three types of Pt–Pt bond in this model are as follows: surface–surface = 0.13, surface–bulk = 0.12, bulk–bulk = 0.12. Pt is a d¹⁰ transition metal. The electron density at each Pt in the surface and bulk layers is computed as 10.06 and 9.88, respectively. The d band of Pt spans the energy range of –11 to –14 eV, with the calculated Fermi energy around –11 eV.

The bond length of a free oxygen molecule in the gas phase is 1.208 Å.[11b] Its molecular orbitals are displayed in Figure 1. Note that the degenerate 1πₛ orbitals are half-filled. Mulliken overlap populations unfortunately do not have the simplistically desired values of chemical bond orders 0, 1, 2, 3, ... For O₂, the OP value which we calculate, 0.80, is a rough measure of a double bond. At an O–O distance of 1.32 Å, the OP calculated is 0.67. Upon chemisorption, the local symmetry of the composite system, which is C_{2v}, is lower than that of the free molecule. Thus, the orbitals need to be labeled differently. The notation for 1πᵤ becomes πᵧ and πᵤ. Similarly, 1πₛ becomes π*ᵧ and π*ᵤ. For simplicity, 3σᵤ will be called σ*. To reveal the basic picture of how oxygen is bonded to different sites, a coverage of 0.25 ML is used, minimizing interaction between the adsorbates. Chart II shows three possible geometries of the first layer on the surface.

Chemisorption of O₂

Figure 2 shows the density of states plots for the on-top and 2-fold site in a selected energy window. The plot for the 3-fold case is very similar to that of on-top and 2-fold,

(19) Chan, A. W. E.; Hoffmann, R. *J. Chem. Phys.* **1990**, *92*, 699.
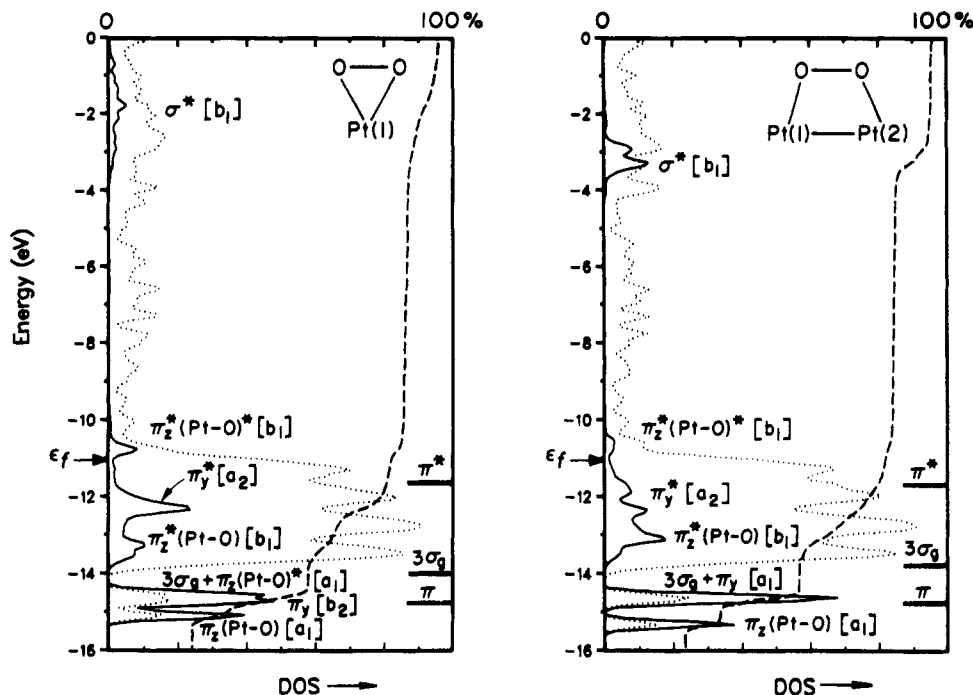
Figure 2. Total density of states (dotted lines) of adsorbed O_2 at the on-top (at left) and bridge (at right) sites on Pt(111), with projected DOS of O_2 states (magnified 3× in solid line) and the integration curves (dashed lines), which are the integrations of the occupation of the projection (all the O_2 states), on a scale of 0–100% given at top. The bars at the right of each window denote the energy of the molecular orbitals of a free O_2 with an O–O distance of 1.208 Å. Symmetry label of specified orbital is listed in brackets.

so it will not be shown here. The $2\sigma_u$ state is outside this energy window. In the free molecule, σ^* is located at +6.73 eV. It has come down about 7 and 9 eV for the on-top and 2-fold sites, respectively. In one of the recent NEXAFS studies, a shift of about 5 eV of the σ^* resonance is found upon chemisorption of O_2.[91]

One expected feature of the interaction is that the degeneracy of the π-type orbitals has now been removed. For example, the π^*_z level splits into bonding [π^*_z(Pt–O)] and antibonding [π^*_z(Pt–O)*] states. These bonding and antibonding Pt–O states are clearly seen in the crystal orbital overlap population (COOP) plots in Figure 3a. These states now span the energy range between –10 and –14 eV. In both sites, $3\sigma_g$ and π are lowered by about 0.5 eV.

The binding energy and several overlap populations are collected in Table II. Judging from the binding energy, the stabilization of chemisorbed molecular oxygen can be seen to fall off in the following sequence: 2-fold, 3-fold, and on-top.

The O–O OP's for all three sites after adsorption are in the range of 0.48–0.55, smaller than in the free molecule (compare to OP = 0.67 even when O–O = 1.32 Å). The chemisorption indeed weakens the O–O bond to some extent. Apparently it is not safe to gauge which site would be better for dissociating O_2 by the overlap population. While the O–O OP is smallest for the site with greatest binding energy, there is a discrepancy between the on-top and 3-fold binding energies and the degree of O–O bond weakening at these sites.

The weakening of the oxygen bond is directly related to the population of the π^* level. Upon chemisorption, π^* gains about 1.41, 1.59, and 1.00 electrons for on-top, 2-, and 3-fold sites, respectively. Let us take a closer look at the π^* levels: actually π^*_z gains 0.42, 0.62, and 0.50 electrons while π^*_y gains about 0.99, 0.97, and 0.50 electrons for the on-top, 2-, and 3-fold sites, respectively. π^*_y is parallel to the surface; it interacts little with the surface in the on-top or 2-fold site. For example, in the on-top

site, π^*_y can only interact with Pt d_{xy} orbital. However, their overlap, S_{ij}, which is only 0.03, is poor (compared with $S_{(Ptd_{xz}|\pi^*_z)} = 0.11$). The corresponding (Pt(d_{xy}–π^*_y)) overlap population is near zero. (Note that OP is proportional to $\sum c_i c_j S_{ij}$, where c_i are the coefficients of the atomic orbital i.) Since π^*_y is located beneath the Fermi level, electrons are transferred into this level as an electron sink. π^*_y in the 3-fold site does not receive as many electrons as in the other sites because it can interact with Pt in the 3-fold symmetry. Some of the states are then pushed up above the Fermi level.

π^*_z interacts well with the surface (as will be described later); the level splits into bonding and antibonding components with respect to the Pt surface states (see Figure 3a). σ^* does gain some electrons but insufficiently so to weaken the O–O bond. σ^* gains 0.02, 0.01, and 0.03 electrons and its O–O OP contributes 2% to the total O–O OP in each of the on-top, 2-, and 3-fold sites. These electrons are drawn from the surface Pt atom. The Pt atom which is directly bound to the adsorbate has indeed lost some electron density (see Table II). The electron density of the bulk layer remains the same as in the clean surface.

Suppose a Pt–O OP of approximately 0.2 (see earlier discussion of model compound) constitutes a regular Pt–O bond, then we may estimate that there are two strong Pt–O bonds in the 2-fold site and two weaker bonds in the on-top site. In the 3-fold site, the value and the number of the Pt–O OP indicates a resemblance to a superposition of the on-top plus 2-fold sites: two strong bonds with Pt(1) and Pt(2) (bridging O_2), and two weaker bonds with Pt(3) (an atop O_2). The greater number of Pt–O bonds in the 3-fold site is seemingly contradictory to the calculated binding energy, which indicates that the 3-fold site is not the most favorable one. The Pt–Pt surface bonds as shown in Table II, are not affected much in the on-top site (compared to 0.13 for the clean surface). However, they are severely weakened in the 3-fold site. A similar argument was given in a study of the chemisorp-
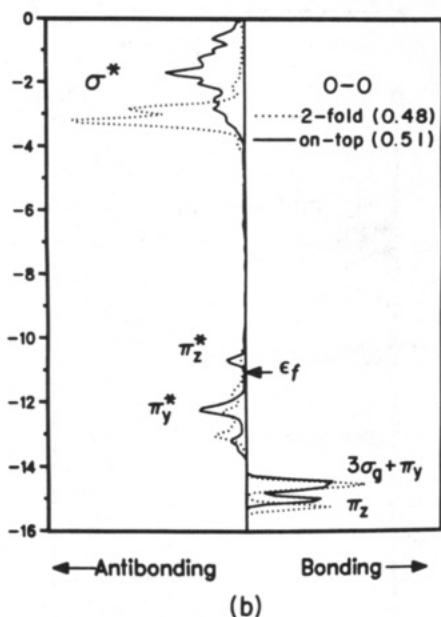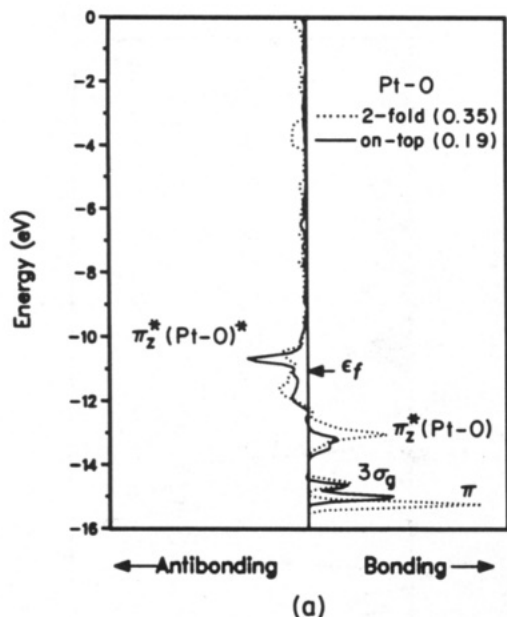
Figure 3. (a) Pt–O crystal orbital overlap population curves in the on-top and 2-fold sites on Pt(111). (b) O–O crystal orbital overlap population curves in the on-top and 2-fold sites on Pt-(111).

Table II. Calculational Results for the Chemisorption of O₂ on Pt(111) in Different Adsorption Sites

adsorption site	on-top	2-fold	3-fold
BE (eV)	2.96	4.21	3.41
overlap populations			
O–O	0.51	0.48	0.55
Pt1–Pt2	0.12	0.10	0.07
Pt1–O	0.19	0.35	0.33
Pt3–O			0.18
Pt1–$2\sigma_u$	0.02 (11%)[a]	0.10 (29%)	0.10 (29%)
Pt1–π_z	0.07 (40%)	0.04 (12%)	0.02 (5%)
Pt1–$3\sigma_g$	−0.01 (−7%)	0.07 (21%)	0.06 (17%)
Pt1–π^*_z	0.09 (46%)	0.11 (31%)	0.06 (17%)
Pt1–π^*_y	0.00 (0%)	0.01 (1%)	0.07 (20%)
net charges of O₂	−1.15	−1.13	−0.37
electron gain for π^*	1.41	1.59	1.00
Electron Density Changes[b] for Pt1 Relative to the Clean Surface			
Pt1	1.28	−0.58	−0.45
p_x	0.05	0.01	0.01
p_z	0.10	0.13	0.09
d_{z^2}	−0.44	−0.50	−0.17
d_{xz}	−0.87	−0.18	−0.11
d_{yz}	−0.01	0.00	−0.25

[a] Percentage of the totel Pt–O overlap population. [b] A negative value indicates electron density being donated to the adsorbate.

Figure 4. Examples of Pt–O bonding in the on-top and 2-fold sites. The numbers are the respective contributions to the overlap populations.

tion of acetylene on Pt(111).[20] The stabilization of chemisorbed systems is a compromise between better Pt–O bonding and less weakened Pt surface bonds.
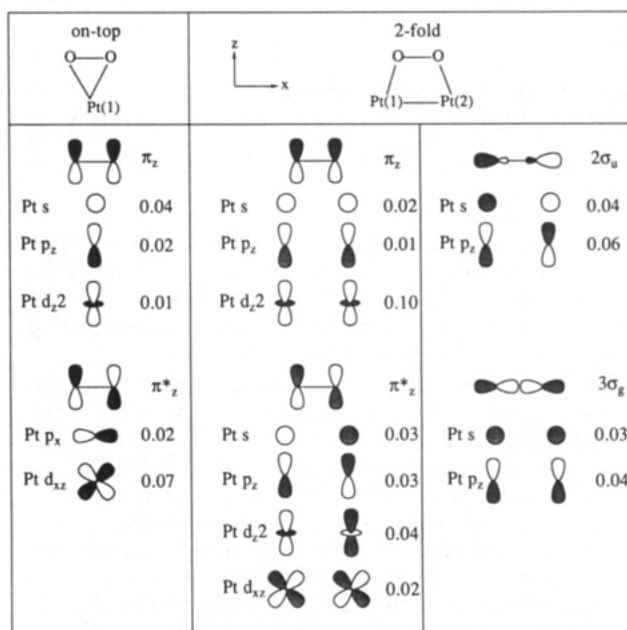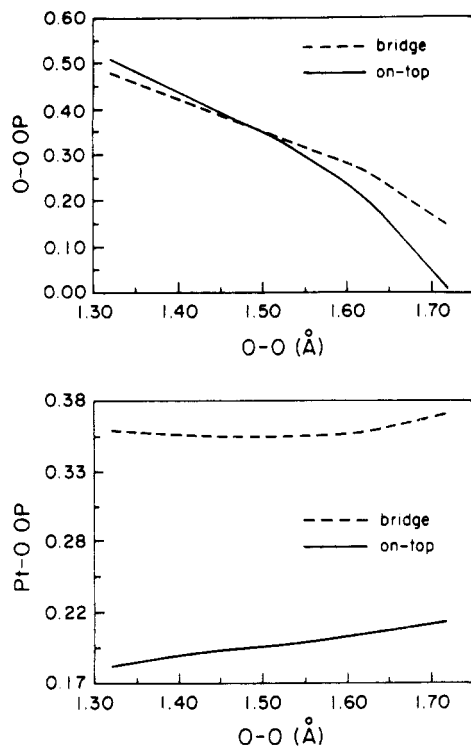
Some typical interactions important in the Pt–O bonding in the on-top and 2-fold sites are depicted in Figure 4. The overlap populations between the specified orbitals [Pt-(atomic orbital)–O₂(FMO)] are listed besides the drawings (FMO denotes fragment molecular orbital). In the on-top site, the bonding picture is quite simple; the interaction with Pt is mainly through the π_z orbitals mixing with the Pt s, p_z and d_{z^2} bands, and π^*_z orbitals with the Pt p_x and d_{xz} bands.

Actually, the overlap populations of π_z and π^*_z in these two sites are comparable for both surfaces (OP = 0.16 and 0.15 for on-top and bridge sites, respectively). However the O₂ $2\sigma_u$ and $3\sigma_g$ are actually responsible for the extra

(20) (a) Silvestre, J.; Hoffmann, R. *Langmuir* **1985**, *1*, 621. (b) Silvestre, J.; Hoffmann, R. *J. Vac. Sci. Technol., A* **1986**, *4*, 1336.

stabilization in the 2-fold site. The big lobes of the $2\sigma_u$ molecular orbitals are pointing outward, directly at the two Pt atoms in 2-fold symmetry, interacting most effectively with Pt s and p_z orbitals. On the other hand, $2\sigma_u$ interacts poorly at the on-top site because it can only mix weakly with the Pt d_{xz} or p_x band (picture not shown here). The same conclusions may be drawn from the electron density shifts, of which a selection at Pt(1) is listed in Table II.

Dissociation and Desorption of O₂ on Pt(111)

Since the Pt–O bonding picture at the 3-fold site is similar to that of on-top and 2-fold, we will just concentrate on the later two sites. The above analysis reflects that it may be harder to break the Pt–O bond in the 2-fold site than in the on-top site. However, it does not provide insights into how the O–O bond is broken. When oxygen
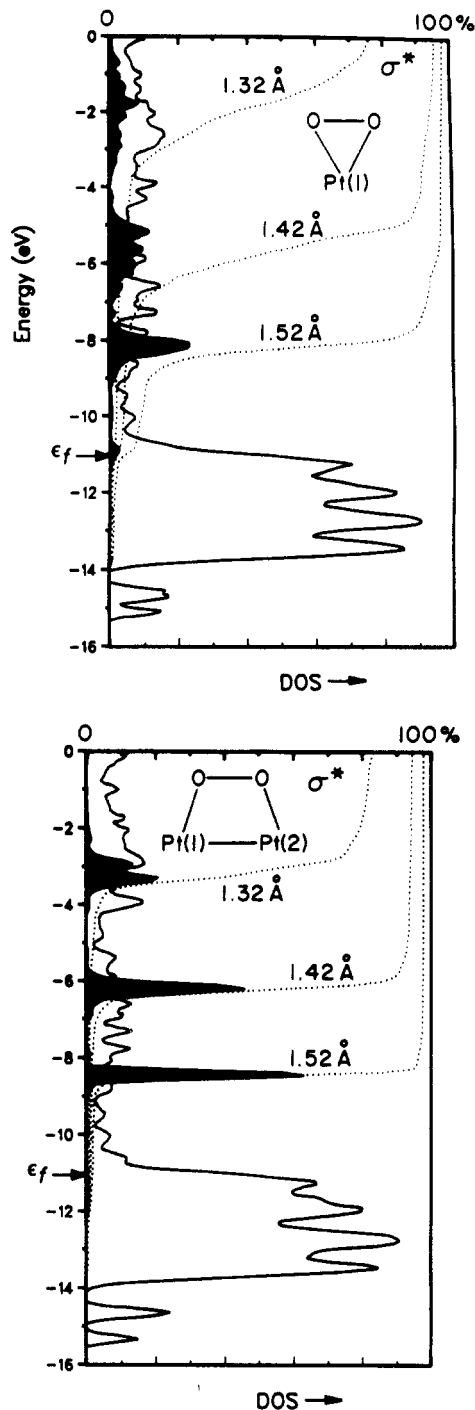
Figure 5. (a) O–O overlap population as a function of O–O distance for O_2 chemisorption in the on-top and 2-fold sites on Pt(111). (b) Pt–O overlap population as a function of O–O distance for O_2 chemisorption in the on-top and 2-fold sites on Pt(111).

is adsorbed, electrons fill up the π^* levels. As the O–O bond is weakened, this will lead to some stretching of the O–O distance. The O–O bond is elongated and the calculation was repeated. Figure 5a shows the O–O overlap population as a function of the O–O distance.

The overlap population diminishes toward zero when O–O is around 1.7 Å. By comparison of the slope of the overlap population curves, the bond strength of O–O at the on-top site is diminishing quicker (but not by much) than that at the 2-fold site. It is difficult to distinguish from this result which site is more favorable in the dissociation reaction. Another interesting feature is that the Pt–O bond for the on-top site is now increasing (0.186 to 0.197) while that of the 2-fold site is decreasing slightly (0.354 to 0.352), although the effect is small (see Figure 5b). The dissociation and desorption reactions may be competing in the 2-fold site. In addition, since the values of Pt–O OP remain almost constant, O atoms will be bonded to the Pt atoms after the dissociation reaction.

Correlations of these effects to changes in the orbitals can be examined. The evolution of the σ^* orbitals at three selected O–O distances, 1.32, 1.42, and 1.52 Å, for both sites is shown in Figure 6. The levels are projected and their integration curves (the integrations of the occupation of all the O_2 states, on a scale of 0–100% given at the top of the graph) are drawn in dotted lines. As the O–O bond is stretching, the σ^* level comes down in energy, resulting in better energy match and interactions with the Pt bands. Not only O_2 π^* but also σ^* are ultimately involved in the dissociation reaction.

The σ^* peaks in the on-top site are broader than those at the 2-fold site, an indication of more interaction with the surface. The electron density of the σ^* orbitals can be reexamined here in the sequence from 1.32 to 1.52 Å: 0.02, 0.03, 0.07 and 0.01, 0.02, 0.04 for on-top and 2-fold sites, respectively. There are more electrons occupying

Figure 6. Evolution of O_2 σ^* orbitals (magnified 5× and shaded in dark) as a function of O–O distance for O_2 chemisorption in the on-top and 2-fold sites on Pt(111). The O–O distance is specified. The solid line represents the total DOS and the dotted line shows the O_2 integrated DOS.

the σ^* in the on-top site. Better Pt-σ^* bonding will correspond to lowering of the σ^* level; the result being a bigger Pt–O OP but a weaker O–O bond in the on-top site. In the 2-fold site, the reason for the weakening of both the O–O and Pt–O bonds is to be found in the π^*_z level, as we have discussed earlier. The (Pt–O π^*_z) OP decreases from 0.11 to 0.10 as the bond distance varies. In summary, it is difficult to decide between the on-top and 2-fold sites with respect to the favored site for dissociation.

In still another approach to the problem, the contributions of O–O OP from π^*_z and σ^* are drawn in Figure 7. Note that both π^*_z and σ^* have the same symmetry,
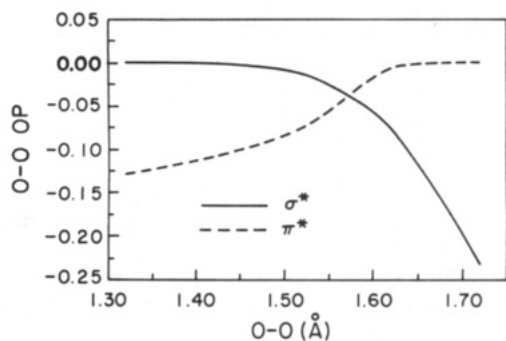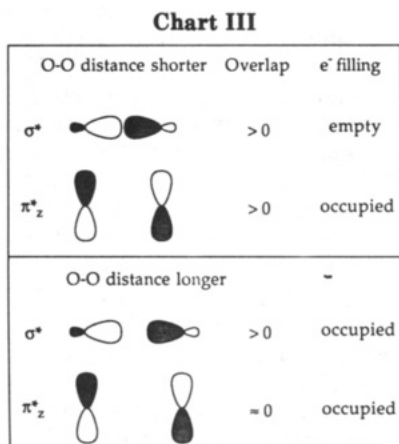
Figure 7. Partition of O_2 π^*_z, σ^* O–O OP contributions to the total O–O OP for the on-top site.

Chart III

Chart IV

Chart V

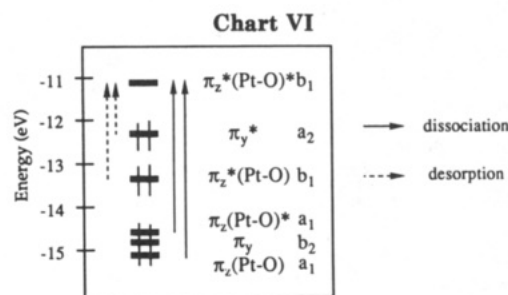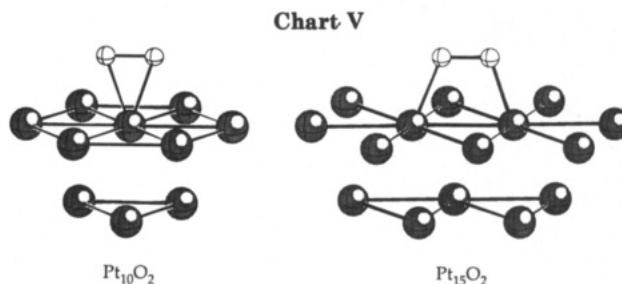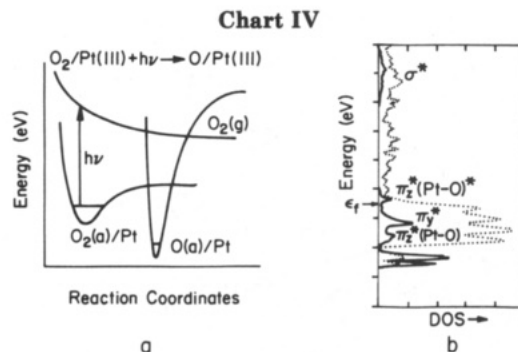$Pt_{10}O_2$ $Pt_{15}O_2$

Chart VI

b_1. Both are O–O antibonding orbitals, therefore contributing a negative value to the total OP. Even if the two levels are of the same symmetry, their O–O OP contribution may be decomposed in terms of atomic orbitals: s, p_x for σ^* and p_z for π^*_z. The dotted line starting at zero for short O–O distance represents the s and p_x contribution to σ^*. This value becomes more negative as the O–O distance increases. The dashed line starting at negative value represents the p_z contribution to π^*_z. This becomes less negative at increasing O–O separation. To understand the calculated trend, Chart III is useful.

When the O–O distance is still small, e.g. 1.32 Å, some of the π^*_z states are below the Fermi level (see Figure 3b). Both σ^* and π^*_z are antibonding orbitals. Therefore, these states contribute a negative value to the O–O OP. As the O–O distance increases, the overlap between these two O p_z orbitals is decreasing. Therefore, even though these states are filled with electrons, the O–O OP values they contribute are less negative (less antibonding). It reaches zero at 1.72 Å. On the other hand, the σ^* orbital is mainly composed of two O p_x orbitals; their overlap is very big and remains substantial even at a longer O–O distance (1.72 Å). When the O–O distance is small, the σ^* states will not contribute anything to the O–O OP, since they are not filled. However, as O–O stretches, σ^* comes down in energy. Electrons fill it and give a negative value to the O–O OP.

For the following discussion, some general points of group theory need to be mentioned. The local geometry of O₂ chemisorption in the on-top and 2-fold sites is C_{2v}.[21] The general selection rule for a dipole allowed electronic

transition is $\langle \Psi_i | r | \Psi_f \rangle \neq 0$. The integrand of this matrix element must be totally symmetric. In C_{2v} symmetry, only the two transitions involving the following symmetries are not allowed: $a_1 \leftrightarrow a_2$ and $b_1 \leftrightarrow b_2$.

The Franck–Condon principle[22] states that an electronic transition occurs so rapidly in comparison with vibrational frequencies that no change in internuclear separation occurs during the course of a transition. For example, in the dissociation process, a schematic potential surface diagram could be drawn as in Chart IV, part a. The excitation energy may be roughly mapped onto the energy difference between different projected states given in the DOS plot in Chart IV, part b.

We begin by setting up two molecular models, $Pt_{10}O_2$ and $Pt_{15}O_2$, to represent the on-top and 2-fold adsorbed O₂. They are shown in Chart V. We assume that the geometry of the excited state is the same as the ground state because of the Franck–Condon principle. An electron is then promoted artifically from an occupied level to an empty one, within the general level scheme of Chart VI. Then, the Pt–O and O–O overlap populations are compared.

The results from one of our cluster models, $Pt_{10}O_2$, are shown in Chart VII. Only the Pt directly bonded to the O₂ is shown in the picture. Note that according to Chart VI, only the π^*_z(Pt–O)* ← π_y transition is not allowed (b_1 ← b_2). All the others are allowed based on the selection rule discussed above. For the ground-state structure, the OP's for Pt–O and O–O are 0.21 and 0.52, respectively. The values are quite close to the numbers that were

(21) The geometry of the adsorbate–substrate complex is C_s. However, the molecular levels involved in the adsorbate–metal bonding as well as the excitation are very localized between the adsorbate and the first layer of the surface. Therefore, both in the discussion and later in the cluster calculations, the C_{2v} local geometry between the adsorbate and the first layer of the surface is used.
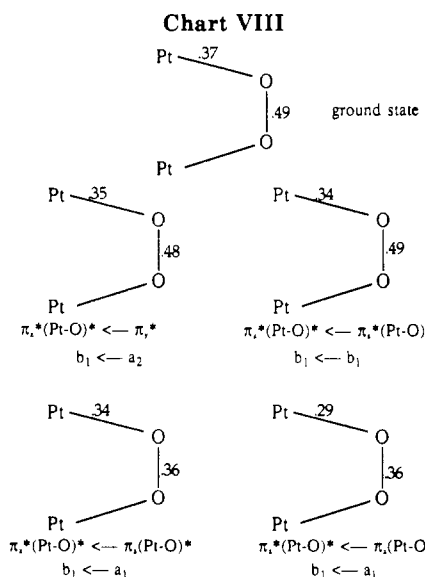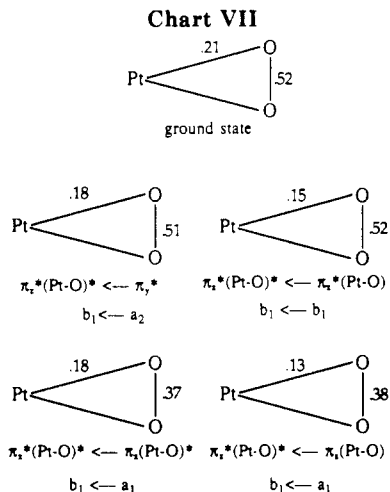
(22) Wayne, R. P. in *Principles and Applications of Photochemistry*; Oxford University Press: New York, 1988.

Chart VII

ground state

$\pi_z*(\text{Pt-O})* \longleftarrow \pi_y*$
$b_1 \longleftarrow a_2$

$\pi_z*(\text{Pt-O})* \longleftarrow \pi_z*(\text{Pt-O})$
$b_1 \longleftarrow b_1$

$\pi_z*(\text{Pt-O})* \longleftarrow \pi_z(\text{Pt-O})*$
$b_1 \longleftarrow a_1$

$\pi_z*(\text{Pt-O})* \longleftarrow \pi_z(\text{Pt-O})$
$b_1 \longleftarrow a_1$

Chart VIII

ground state

$\pi_z*(\text{Pt-O})* \longleftarrow \pi_y*$
$b_1 \longleftarrow a_2$

$\pi_z*(\text{Pt-O})* \longleftarrow \pi_z*(\text{Pt-O})$
$b_1 \longleftarrow b_1$

$\pi_z*(\text{Pt-O})* \longleftarrow \pi_z(\text{Pt-O})*$
$b_1 \longleftarrow a_1$

$\pi_z*(\text{Pt-O})* \longleftarrow \pi_z(\text{Pt-O})$
$b_1 \longleftarrow a_1$

obtained from the solid-state calculations. The O–O OP's of $\pi_z*(\text{Pt-O})* \longleftarrow \pi_z*(\text{Pt-O})$ and $\pi_z*(\text{Pt-O})* \longleftarrow \pi_y*$ excitations do not change much, relative to the ground state. However, the $\pi_z*(\text{Pt-O})* \longleftarrow \pi_z(\text{Pt-O})*$, and $\pi_z*(\text{Pt-O})* \longleftarrow \pi_z(\text{PtO})$ excitations all lead to a decrease in O–O OP. Therefore, these two excitations would be very good candidates for the dissociation reaction, within these models.

In Figure 2a, for the dissociation reaction, the first direct excitation of the adsorbate–substrate complex probably involves electrons transferring into the $\pi_z*(\text{Pt-O})*$ level (b_1) from an occupied level. For electron transfer from $\pi_z(\text{Pt-O})*$ and $\pi_z*(\text{Pt-O})$ into $\pi_z*(\text{Pt-O})*$ of the adsorbate–substrate complex, the energy is 3.5 and 4.2 eV, respectively. Mieher and Ho have reported a 2.5-eV threshold energy for the photodissociation of O_2.[2a] Zhu, Hatch, Campion, and White[9c] have determined that the photodissociation is negligible at wavelength > 300 nm (≈4 eV). As we discussed above, the breaking of the O–O bond can also arise from occupation of the $\sigma*$ level. The range of energy that is required to excite an electron from near the Fermi level to $\sigma*$ will be between 7.5 and 11.5 eV. The electron stimulated desorption experiment done by Orlando, Burns, Stechel, and Jennison has also observed a 8–10-eV threshold for the dissociation of O_2 on Pt(111).[23] All the above three mechanisms are possible. For photon

(23) Orlando, T. M.; Burns, A. R.; Stechel, E. B.; Jennison, D. R. *J. Chem. Phys.* **1990**, *93*, 9197.

Table III. Extended Hückel Parameters

atom	orbital	H_{ii}, eV	ζ_1	ζ_2	$c_1{}^a$	$c_2{}^a$
Pt	6s	−8.94	2.55			
	6p	−5.37	2.55			
	5d	−12.36	6.01	2.696	0.6333	0.5512
O	2s	−29.60	2.27			
	2p	−13.60	2.27			

[a] Coefficients used in the double-ζ expansion of the d orbitals.

energies in the range from 2 to 6 eV, direct electronic excitation of the adsorbate–substrate complex is the most likely mechanism for O_2 on Pt(111).

We discuss next the desorption of O_2. If we look at the Pt–O COOP curve again in Figure 3a, the Pt–O antibonding states are located just above the Fermi level, so excitation of an electron into this level will enhance the reaction. In molecular desorption, the Pt–O bond should be weakened but not necessarily the O–O bond. From the information in Chart VII, two of the transitions satisfy these requirements. Both $\pi_z*(\text{Pt-O})* \longleftarrow \pi_y*$ and $\pi_z*(\text{Pt-O})* \longleftarrow \pi_z*(\text{Pt-O})$ weaken the Pt–O bond, but the latter one seems to have a slightly greater effect. The excitation energies required for these two transitions measured from Figure 2a are 1.5 and 2.5 eV, respectively.

Now let us turn to the 2-fold site model, $Pt_{15}O_2$. Our computational results are shown in Chart VIII. Basically these results are very similar to those of the on-top model in terms of energetics of the molecular levels. The same arguments for dissociation and desorption mentioned in the previous paragraph will be used again. Desorption is indicated by the first two transitions as displayed in Chart VI, $\pi_z*(\text{Pt-O})* \longleftarrow \pi_y*$ and $\pi_z*(\text{Pt-O})* \longleftarrow \pi_z*(\text{Pt-O})$, while dissociation is more likely from the last two excitations, $\pi_z*(\text{Pt-O})* \longleftarrow \pi_z(\text{Pt-O})*$ and $\pi_z*(\text{Pt-O})* \longleftarrow \pi_z(\text{Pt-O})$. However, the latter transition has a bigger effect.

Summary

It should be stressed again that the extended Hückel method tends to overestimate the binding or excitation energy. The values reported here can only serve as a guide, perhaps as an upper bound relative to the experimental data. However, this approximate molecular orbital method seems to capture the essence of bonding, which is useful in constructing explanations.[7,24] Our arguments thus are mostly based on symmetry and overlap populations, as discussed in the text.

Our calculations indicate that in the chemisorption of O_2, the O–O bond strength does not change much in the three different sites. The strength of the bonding between $2\sigma_u$, $3\sigma_g$ and the metal surface favors a higher coordination site, while the $\pi*_z$ interaction changes only slightly in various adsorption sites. In the 3-fold site, the Pt–O bonding picture is a superposition of that of on-top and 2-fold sites. Pt–O bonding is counterbalanced by weakening of the Pt–Pt surface bonds. In our analysis of the photodissociation, it is a one-step process. As the O_2 $\pi*$ becomes occupied by electrons, the O–O bond is stretched. Simultaneously, the $\sigma*$ orbital is gradually moving down, to be eventually filled by electrons. Desorption is attributed to a $\pi*_z(\text{Pt-O})$ to $\pi*_z(\text{Pt-O})*$ excitation of the adsorbate–substrate complex. The photoinduced desorption and dissociation of O_2 on Pt(111) proceed via direct electronic excitation of the adsorbate–substrate complex.

(24) Hoffmann, R. *Rev. Mod. Phys.* **1988**, *60*, 601.

Appendix

The tight binding extended Hückel method[25] was used for all the calculations. The extended Hückel method's valence state ionization potentials for the O and Pt atoms are obtained by charge iteration.[26] They are listed in Table III.

We define a binding energy (BE) as E(slab) + E(adsorbate) − E(composite system). Thus a positive BE indicates stabilization.

A set of 18k points was used in all the surface calculations.

(25) (a) Hoffmann, R.; Lipscomb, W. N. *J. Chem. Phys.* **1962**, *36*, 2179; **1962**, *37*, 2872. (b) Hoffmann, R. *J. Chem. Phys.* **1963**, *39*, 1397.

(26) Ballhausen, C. J.; Gray, H. B. In *Molecular Orbital Theory*; Benjamin: New York, 1965.